

Quantum-Trajectory-Inspired Lindbladian Simulation

Sirui Peng,¹ Xiaoming Sun,¹ Qi Zhao,² and Hongyi Zhou^{1,*}

¹State Key Lab of Processors, Institute of Computing Technology,
Chinese Academy of Sciences, 100190, Beijing, China.

²QICI Quantum Information and Computation Initiative, Department of Computer Science,
The University of Hong Kong, Pokfulam Road, Hong Kong

(Dated: August 21, 2024)

Simulating the dynamics of open quantum systems is a crucial task in quantum computing, offering wide-ranging applications but remaining computationally challenging. In this paper, we propose two quantum algorithms for simulating the dynamics of open quantum systems governed by Lindbladians. We introduce a new approximation channel for short-time evolution, inspired by the quantum trajectory method, which underpins the efficiency of our algorithms. The first algorithm achieves a gate complexity independent of the number of jump operators, m , marking a significant improvement in efficiency. The second algorithm achieves near-optimal dependence on the evolution time t and precision ϵ and introduces only an additional $\tilde{O}(m)$ factor, which strictly improves upon state-of-the-art gate-based quantum algorithm that has an $\tilde{O}(m^2)$ factor. In both our algorithms, the reduction of dependence on m significantly enhances the efficiency of simulating practical dissipative processes characterized by a large number of jump operators.

I. INTRODUCTION

Simulating physical systems using quantum-mechanics-based computational devices [1] is a foundational motivation for developing quantum computers. Traditionally, most quantum algorithms have primarily focused on the Hamiltonian dynamics of closed systems, assuming no interaction with the environment. In contrast, the paradigm of open quantum systems incorporates environmental effects, offering a more realistic depiction of real-world systems, albeit at the cost of increased computational complexity. A widely studied case is the Markovian open quantum system, which can describe many practical quantum systems through operators acting solely on the system itself. Studying the evolution of open systems has crucial applications in quantum chemistry [2, 3], quantum physics [4], and even mathematical optimization [5].

The evolution of a Markovian open system is governed by the Lindblad master equation (LME):

$$\begin{aligned} & \frac{d\rho(t)}{dt} \\ &= -i[H, \rho(t)] + \sum_{\alpha=1}^m \left(L_{\alpha}\rho(t)L_{\alpha}^{\dagger} - \frac{1}{2} \{L_{\alpha}^{\dagger}L_{\alpha}, \rho(t)\} \right) \quad (1) \\ &= \mathcal{L}\rho(t), \end{aligned}$$

where \mathcal{L} is the Lindbladian, H is the system Hamiltonian, and m jump operators L_1, \dots, L_m representing environmental effects. Our goal is to construct circuits that implement a channel \mathcal{N} such that $\|\mathcal{N} - e^{\mathcal{L}t}\|_{\diamond} \leq \epsilon$ for a given Lindbladian \mathcal{L} , evolution time t , and precision ϵ .

There has been increasing interest in open quantum system simulation in recent years. The first efficient

algorithm with exponentially small precision was proposed by Childs and Wang [6], achieving a gate cost of $O(m^2 t \text{poly} \log(m^2 t/\epsilon))$. Li and Wang [7] further explore simulating Lindbladian using higher series expansion, and obtain an efficient algorithm with $O(t \text{poly} \log(t/\epsilon))$ calls of the $m + 1$ block-encoding circuits of the Hamiltonian and jump operators. There are also attempts to reduce Lindbladian simulation to Hamiltonian simulation [8, 9], but these attempts do not achieve the exponential precision dependence. Additionally, there are works considering the sample complexity of Lindbladian simulation [10, 11].

For all methods discussed above, the gate complexity dependence on the number of jump operators m is at least $\Omega(m)$, which can scale exponentially with the qubit number n and thus becomes a huge overhead. Consider an n -qubit system where dissipation occurs through collective lowering operations involving arbitrary subsets of qubits. Such a scenario is representative of systems where qubits are closely spaced and interact with the environment in complex, collective manners. In this context, the jump operators associated with the dissipation can be defined for every possible subset S of qubits as

$$L_S = \sqrt{\gamma_S} \prod_{i \in S} \sigma_i^-, \quad (2)$$

where S is any non-empty subset of $\{1, 2, \dots, n\}$, γ_S is the collective decay rate for the subset S and $\sigma_i^- = |0\rangle\langle 1|_i$ is the lowering operator for the i -th qubit. In such physical systems, the number of jump operators can be as large as $O(4^n)$. Therefore, reducing m -dependence can provide exponential speedup for the simulation of such physical systems.

To solve the problem above, we propose two novel quantum algorithms for the simulation of Markovian open quantum systems, greatly reducing the dependence on the number of jump operators. These algorithms are inspired by the quantum trajectory method in classical

* zhouhongyi@ict.ac.cn

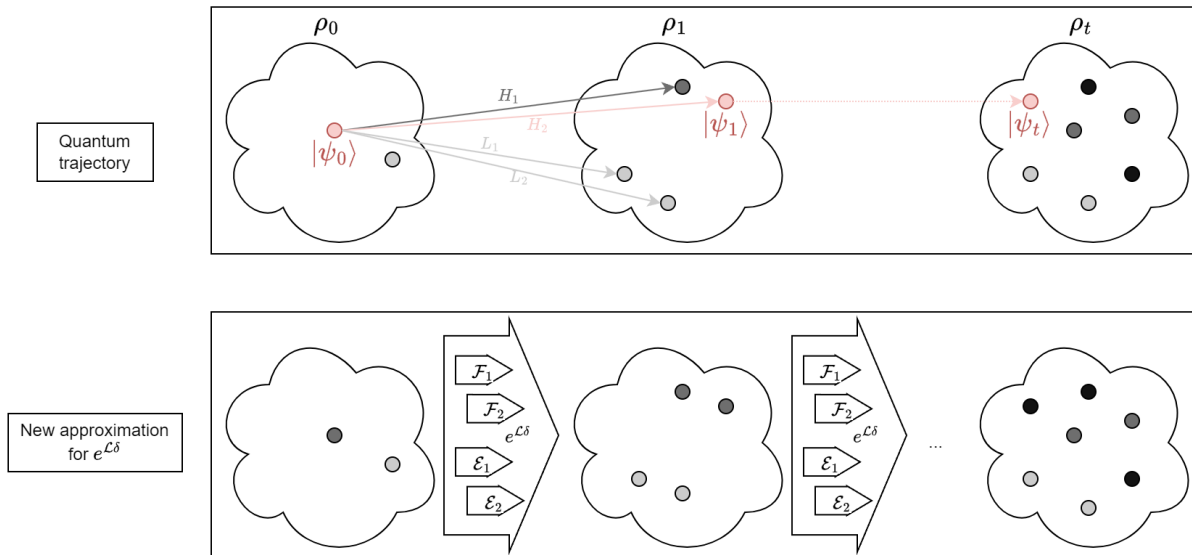


FIG. 1. In quantum trajectory method, the state of the system is viewed as a mixture of pure states, and a trajectory is a sequence of pure states $|\psi_0\rangle, |\psi_1\rangle, \dots, |\psi_t\rangle$, the system states under a possible list of individual evolution operators. In this figure, an example Lindbladian with $H = H_1 + H_2$ and jump operators $\{L_1, L_2\}$ is presented. The mixture of all possible trajectories provides a good approximation of the evolution. Inspired by the quantum trajectory method, we introduce a new approximation for the short-time evolution of LME that is composed of efficiently implementable individual channels. In this figure, the individual channels $\mathcal{F}_1, \mathcal{F}_2$ correspond to individual Hamiltonians H_1, H_2 , and $\mathcal{E}_1, \mathcal{E}_2$ correspond to jump operators L_1, L_2 .

simulations of open systems (see Fig. 1), which enables us to find a new approximation channel for short-time evolution. Algorithm 1 eliminates m -dependence in gate complexity through a simple sampling method. This resembles the qDRIFT algorithm [12] in Hamiltonian simulation, highlighting the power of classical randomness. Algorithm 2 uses a structured LCU method, reducing m -dependence from $\tilde{O}(m^2)$ to $\tilde{O}(m)$ while maintaining near-optimal (t, ϵ) -dependence of $O\left(t \frac{\log^2(t/\epsilon)}{\log \log(t/\epsilon)}\right)$. By reducing the dependence on the number of jump operators, our algorithms address a critical bottleneck in the practical application of quantum computing to real-world problems characterized by complex dissipative dynamics.

II. MAIN RESULTS

We first list our main results and leave the proof in the next sections. We assume that operators within \mathcal{L} are given as linear combinations of q Pauli strings [6],

$$H = \sum_{l=1}^q T_{0l} V_{0l},$$

$$L_j = \sum_{l=1}^q T_{jl} V_{jl}, j = 1, \dots, m, \quad (3)$$

where $T_{jl} \geq 0$ and V_{jl} are Pauli strings. The norm depicting the intensity of \mathcal{L} is defined as:

$$\|\mathcal{L}\|_{\text{pauli}} = \|H\|_{\text{pauli}} + \sum_{j=1}^m \|L_j\|_{\text{pauli}}^2, \quad (4)$$

where $\|H\|_{\text{pauli}} = \sum_{l=1}^q T_{0l}$ and $\|L_j\|_{\text{pauli}} = \sum_{l=1}^q T_{jl}$ for $j = 1, \dots, m$. Also, we use $\|\cdot\|_1$ to denote Schatten 1-norm, $\|\cdot\|_2$ to denote Euclidean norm of a vector, and $\|\cdot\|_{\text{op}}$ to denote spectral norm (i.e. operator norm) for a matrix.

Our main contributions are summarized in the following theorems. We first present a quantum algorithm for Lindbladian simulation removing the m -dependence.

Theorem 1. *Let \mathcal{L} be a Lindbladian presented as a linear combination of q Pauli strings. For any $t > 0$ and $\epsilon > 0$, there exist quantum circuits of gate count*

$$O\left(\frac{qn\tau^2}{\epsilon}\right)$$

such that sampling from these circuits implements a quantum channel \mathcal{N} , with $\|\mathcal{N} - e^{\mathcal{L}t}\|_{\diamond} \leq \epsilon$, where $\tau = t\|\mathcal{L}\|_{\text{pauli}}$.

Additionally, the (t, ϵ) -dependence can be improved to near-optimal at the cost of introducing an $\tilde{O}(m)$ factor.

Theorem 2. Let \mathcal{L} be a Lindbladian presented as a linear combination of q Pauli strings. Then, for any $t > 0$ and $\epsilon > 0$, there exists a quantum circuit of gate count

$$O\left(mq\tau \frac{(\log(mq\tau/\epsilon) + n) \log(\tau/\epsilon)}{\log \log(\tau/\epsilon)}\right)$$

that implements a quantum channel \mathcal{N} , such that $\|\mathcal{N} - e^{\mathcal{L}t}\|_{\diamond} \leq \epsilon$, where $\tau = t\|L\|_{\text{pauli}}$.

Algorithm	Gate count (t, ϵ)	Gate count (m)
Algorithm 1	$O(t^2/\epsilon)$	$O(1)$
Algorithm 2	$O\left(t \frac{(\log(t/\epsilon))^2}{\log \log(t/\epsilon)}\right)$	$O(m \log m)$
Channel LCU scheme [6]	$O\left(t \frac{(\log(t/\epsilon))^2}{\log \log(t/\epsilon)}\right)$	$O(m^2 \log m)$
Hamiltonian reduction (First-order) [9]	$O(t^2/\epsilon)$	$O(m)$
Hamiltonian reduction (k -order, $k > 1$) [9]	$O\left(t \left(\frac{t}{\epsilon}\right)^{1/k}\right)$	$O(m^{k+1})$
RI scheme [8]	$O(t^3/\epsilon)$	$O(m^2)$

TABLE I. Comparison between our results and previous results.

III. NEW APPROXIMATION FOR $e^{\mathcal{L}\delta}$

Our new approximate channel design is inspired by the quantum trajectory method [13–15], an approach to simulating Markovian open quantum system numerically. Recall that in Equation (1), the state of the system is represented by its density matrix $\rho = \sum_j p_j |\psi_j\rangle \langle \psi_j|$, and its evolution is viewed as a deterministic transform from ρ_0 to ρ_t . The quantum trajectory method instead has another perspective. The state of the system is viewed as a mixture of pure states $\{(p_j, |\psi_j\rangle)\}_j$. Each pure state goes through a stochastic process where a random list of individual evolution operators (the Hamiltonian or a jump operator) is applied, and the state of the evolved system is the mixture of all possible result states, i.e. the average of all possible quantum trajectories.

More precisely, the following process shows how to calculate a single trajectory [16] via the first-order quantum trajectory method. This allows for a full simulation since the density matrix of the evolved system can be approximated by averaging over many trajectories.

1. Sample the initial state $|\psi(0)\rangle$ from the initial density operator ρ_0 . Set $x = 0$ and the adequate time step δ .
2. Compute evolved state under effective Hamiltonian $|\phi_0\rangle = (I - i\delta(H - \frac{i}{2} \sum_{j=1}^m L_j^\dagger L_j)) |\psi(x)\rangle$, and its amplitude $\langle \phi_0 | \phi_0 \rangle = p_0$.
3. Compute the evolved state under a single jump operator $|\phi_j\rangle = \sqrt{\delta} L_j |\psi(x)\rangle$, and its amplitude $\langle \phi_j | \phi_j \rangle = p_j$ for $j = 1, \dots, m$.

4. Compute the state

$$|\psi(x + \delta)\rangle = \frac{|\phi_j\rangle}{\sqrt{p_j}}, \text{ w.prob. } p_j, \text{ for } j = 0, 1, \dots, m$$

as state of the next time step. On condition that δ is small enough, $\sum_{j=0}^m p_j \approx 1$.

5. Repeat until $|\psi(t)\rangle$ is obtained for desired evolution time t .

The key observation from the quantum trajectory method is to utilize *classical randomness* and avoid related computational costs by sampling.

In the following lemma, we propose a new approximation channel \mathcal{E} for short-time evolution $e^{\mathcal{L}\delta}$. This channel is the mixture of individual channels that represent the effects of Hamiltonian ($\mathcal{F}_1, \dots, \mathcal{F}_q$) and jump operators ($\mathcal{E}_1, \dots, \mathcal{E}_m$) respectively. In our construction each individual channel is positive and trace-preserving (up to an error of $O(\delta^2)$), and thus can be implemented as individual quantum circuits.

Lemma 1 (quantum trajectory method via quantum channel). Let \mathcal{L} be a Lindbladian presented as a linear combination of q Pauli strings. Let $\lambda = \|\mathcal{L}\|_{\text{pauli}}$ and $c_j = \|L_j\|_{\text{pauli}} = \sum_{l=1}^q T_{jl}$, $j = 1, \dots, m$. Define channels

$$\mathcal{F}_l(\rho) = (I - i\lambda\delta V_{0l})\rho(I - i\lambda\delta V_{0l})^\dagger, \quad l = 1, \dots, q \quad (5)$$

and

$$\mathcal{E}_j(\rho) = A_{j0}\rho A_{j0}^\dagger + A_{j1}\rho A_{j1}^\dagger, \quad j = 1, \dots, m \quad (6)$$

where

$$\begin{aligned} A_{j0} &= I - \frac{\lambda\delta}{2c_j^2} L_j^\dagger L_j, \\ A_{j1} &= \sqrt{\frac{\lambda\delta}{c_j^2}} L_j. \end{aligned} \quad (7)$$

Let

$$\mathcal{E} = \sum_{l=1}^q \frac{T_{0l}}{\lambda} \mathcal{F}_l + \sum_{j=1}^m \frac{c_j^2}{\lambda} \mathcal{E}_j, \quad (8)$$

then

$$\|\mathcal{E} - e^{\mathcal{L}\delta}\|_{\diamond} \leq 5(\lambda\delta)^2. \quad (9)$$

Proof. We apply the result from [6]

$$\|(I + \delta\mathcal{L}) - e^{\mathcal{L}\delta}\|_{\diamond} \leq (\delta\|L\|_{\diamond})^2 \leq (2\lambda\delta)^2. \quad (10)$$

Denote the Hilbert space \mathcal{L} acting on as \mathcal{H} . By definition,

$$\|\mathcal{E} - (I + \delta\mathcal{L})\|_{\diamond} = \max_{Q \in \mathcal{H} \otimes \mathcal{K}} \|(\mathcal{E} \otimes I_{\mathcal{K}} - (I_{\mathcal{H}} + \delta\mathcal{L}) \otimes I_{\mathcal{K}}) Q\|_1, \quad (11)$$

for an arbitrary Hilbert space \mathcal{K} and $Q \in \mathcal{H} \otimes \mathcal{K}$ that $\|Q\|_1 = 1$. Bound the right-hand side and we will have a bound for $\|\mathcal{E} - (I + \delta\mathcal{L})\|_\diamond$. Notice that for $j = 1, \dots, m$,

$$\begin{aligned} & c_j^2(\mathcal{E}_j \otimes I_{\mathcal{K}})Q \\ &= c_j^2 Q + \lambda\delta \left((L_j \otimes I_{\mathcal{K}})Q(L_j \otimes I_{\mathcal{K}})^\dagger - \frac{1}{2}\{L_j^\dagger L_j \otimes I_{\mathcal{K}}, Q\} \right) \\ &+ \frac{\lambda^2 \delta^2}{4c_j^2} (L_j^\dagger L_j \otimes I_{\mathcal{K}})Q(L_j^\dagger L_j \otimes I_{\mathcal{K}}), \end{aligned} \quad (12)$$

and for $l = 1, \dots, q$,

$$\begin{aligned} & T_{0l}(\mathcal{F}_l \otimes I_{\mathcal{K}})Q \\ &= T_{0l}Q - i\lambda\delta[T_{0l}V_{0l} \otimes I_{\mathcal{K}}, Q] \\ &+ T_{0l}\lambda^2\delta^2(V_{0l} \otimes I_{\mathcal{K}})Q(V_{0l} \otimes I_{\mathcal{K}}). \end{aligned} \quad (13)$$

Combining with

$$\mathcal{E} \otimes I_{\mathcal{K}} = \frac{1}{\lambda} \left(\sum_{k=1}^q T_{0k}(\mathcal{F}_k \otimes I_{\mathcal{K}}) + \sum_{j=1}^m c_j^2(\mathcal{E}_j \otimes I_{\mathcal{K}}) \right), \quad (14)$$

we have

$$\begin{aligned} & (\mathcal{E} \otimes I_{\mathcal{K}} - (I_{\mathcal{H}} + \delta\mathcal{L}) \otimes I_{\mathcal{K}})Q \\ &= \lambda\delta^2 \left(\sum_{l=1}^q T_{0l}(V_{0l} \otimes I_{\mathcal{K}})Q(V_{0l} \otimes I_{\mathcal{K}}) \right. \\ &\left. + \frac{1}{4} \sum_{j=1}^m (L_j^\dagger L_j \otimes I_{\mathcal{K}})Q(L_j^\dagger L_j \otimes I_{\mathcal{K}})/c_j^2 \right), \end{aligned} \quad (15)$$

and

$$\begin{aligned} \|\mathcal{E} \otimes I_{\mathcal{K}} - (I_{\mathcal{H}} + \delta\mathcal{L}) \otimes I_{\mathcal{K}}\|_1 &\leq \lambda\delta^2 \left(c_0 + \frac{\sum_{j=1}^m \|L_j\|_1^4}{4c_j^2} \right) \\ &\leq (\lambda\delta)^2. \end{aligned} \quad (16)$$

The last line holds because $\|L_j\|_1 \leq c_j, j = 1, \dots, m$. Combined with Equation (10) we have proved the result. \square

Notice that $\mathcal{F}_l, l = 1, \dots, q$ and $\mathcal{E}_j, j = 1, \dots, m$ are not trace-preserving, but they almost do. For $j = 1, \dots, m+q$

$$\left\| \sum_k A_{jk}^\dagger A_{jk} - I \right\|_1 \leq (\delta\lambda)^2,$$

where $A_{m+l,0} = I - i\lambda\delta V_{0l}$ for $l = 1, \dots, q$.

IV. SIMULATION VIA SAMPLING

A natural way of implementing \mathcal{E} is by sampling from implementations of these individual channels, which removes the dependence on the jump operator number m . Combined with the algorithmic technique of oblivious amplitude amplification for isometries (Lemma 2 in [6]), we propose Algorithm 1 for Lindbladian simulation, and analyze its approximation error and gate complexity.

A. Individual channel simulation gadget

All quantum channels can be expressed as the partial trace of a unitary operation in a larger Hilbert space, a process known as purification. Extending this notion, we define "probabilistic purification". It is a unitary acting on $\mathcal{H}_{\text{ctrl}} \otimes \mathcal{H}_{\text{sel}} \otimes \mathcal{H}$, and it performs corresponding quantum channel on tracing out selection space \mathcal{H}_{sel} and control space $\mathcal{H}_{\text{ctrl}}$.

Definition 1. Given a channel $\mathcal{G}(\rho) = \sum_{j=1}^g A_j \rho A_j^\dagger$, the probabilistic purification of \mathcal{G} is a unitary $U_{\mathcal{G},p}$ satisfying

$$U_{\mathcal{G},p} |0\rangle_{\text{ctrl}} |0\rangle_{\text{sel}} |\psi\rangle = \sqrt{p} |0\rangle_{\text{ctrl}} \left(\sum_{j=1}^g |j\rangle_{\text{sel}} A_j |\psi\rangle \right) + |\perp\rangle, \quad (17)$$

where $|\perp\rangle$ is orthogonal to the subspace of the control register in the state $|0\rangle$, i.e. $\text{tr}(|0\rangle\langle 0|_{\text{ctrl}} \otimes I_{\text{sel}} \otimes I) |\perp\rangle \langle \perp| = 0$, and p is called the purification probability.

Once we can construct a probabilistic purification circuit, we can perform the corresponding quantum channel. Next we show $\{\mathcal{F}_1, \dots, \mathcal{F}_q, \mathcal{E}_1, \dots, \mathcal{E}_m\}$ have probabilistic purification circuits with probability $p = 1 - 2\lambda\delta$.

First, we consider the simulation of \mathcal{F}_l .

Lemma 2. Probabilistic purification of \mathcal{F}_l with purification probability $p = 1 - 2\lambda\delta$ can be implemented with $O(n)$ gates for $l = 1, \dots, q$.

Proof. Let

$$R_\alpha = \frac{1}{\sqrt{\cos \alpha + \sin \alpha}} \begin{bmatrix} \sqrt{\cos \alpha} & \sqrt{\sin \alpha} \\ \sqrt{\sin \alpha} & -\sqrt{\cos \alpha} \end{bmatrix}.$$

Circuit 2 performs the map

$$|0, 0\rangle_{\text{ctrl}} |\psi\rangle \mapsto \sqrt{q_{\alpha, \beta_1}} |0, 0\rangle_{\text{ctrl}} (I - iV_{0l} \tan \alpha) |\psi\rangle + |\perp\rangle$$

for some state $|\perp\rangle$ orthogonal to the subspace of $|0, 0\rangle_{\text{ctrl}}$, and $q_{\alpha, \beta_1} = \frac{1}{(1+\tan \alpha)^2 (1+\tan \beta_1)^2}$.

Suppose $\beta = 0$. Let $\alpha = \arctan \lambda\delta$, then the circuit implements a probabilistic purification of \mathcal{F}_l with purification probability $p_1 = \frac{1}{(1+\lambda\delta)^2} > 1 - 2\lambda\delta = p$. The second control qubit and rotation gate R_{β_1} with $\beta_1 = \arctan \left(\sqrt{\frac{p_1}{p}} - 1 \right)$ would tune the purification probability to p .

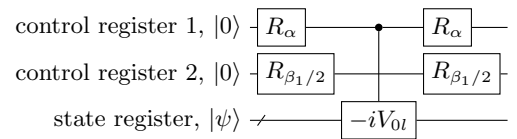


FIG. 2. Gadget circuit for simulating \mathcal{F}_l modified from [17]. \square

Considering the simulation of \mathcal{E}_j , its Kraus operators are highly structured. Therefore, it is possible to simulate \mathcal{E}_j by using a nested LCU circuit that costs only $O(qn)$, while the general LCU method [6] costs $O(q^2n)$ in this scenario. Intuitively, we create L_j conditioning on the selection register being $|0\rangle$. On selection register being $|1\rangle$, we first create $-L_j^\dagger L_j$, and then create its linear combination with the identity operator I . We tweak the rotation gates on the selection register and the first control register to implement the correct coefficients.

Lemma 3. *Probabilistic purification circuit of \mathcal{E}_j with purification probability $p = 1 - 2\lambda\delta$ can be implemented with $O(qn)$ gates for $j = 1, \dots, m$.*

Proof. Define $U_j = \{V_{jl}|l = 1, \dots, q\}$, $-U_j = \{-V_{jl}|l = 1, \dots, q\}$ and $U_j^\dagger = \{V_{jl}^\dagger|l = 1, \dots, q\}$. Figure 4 depicts a set of binary-controlled unitary matrices.

Circuit 3 represents selection space with one register (selection register), and control space with four registers (control register 1, 2, 3, 4). Let us ignore control register 1 for now. The circuit maps the initial state $|0\rangle_{\text{sel}}|0\rangle_{\text{ctrl}}|\psi\rangle$ to

$$\begin{aligned} & \sqrt{p_{\alpha_1, \alpha_2}} \left[|1\rangle_{\text{sel}} |0\rangle_{\text{ctrl}} (1 + \tan \alpha_2) \sqrt{\tan \alpha_1} \frac{L_j}{c_j} |\psi\rangle \right. \\ & \left. + |0\rangle_{\text{sel}} |0\rangle_{\text{ctrl}} \left(I - \tan \alpha_2 \frac{L_j^\dagger L_j}{c_j^2} \right) |\psi\rangle \right] \\ & + |\perp\rangle, \end{aligned} \quad (18)$$

where

$$p_{\alpha_1, \alpha_2} = \frac{1}{(\tan \alpha_2 + 1)^2 (\tan \alpha_1 + 1)}, \quad (19)$$

and $|\perp\rangle$ is orthogonal to the subspace of $|0\rangle_{\text{ctrl}}$. By setting $\alpha_1 = \arctan\left(\frac{\lambda\delta}{(1+\lambda\delta/2)^2}\right)$ and $\alpha_2 = \arctan\frac{\lambda\delta}{2}$, Circuit 3 (without control register 1) implements probabilistic purification of \mathcal{E}_j with purification probability $p_2 = \frac{1}{\lambda\delta + (1+\lambda\delta/2)^2} > 1 - 2\lambda\delta = p$.

Now we take control register 1 back into consideration. With $\beta_2 = \arctan\left(\sqrt{\frac{p_2}{p}} - 1\right)$, it tunes the purification probability to p . \square

By Lemma 2 and 3 we have implemented probabilistic purification circuits $U_{\mathcal{G}, p}$ for $\mathcal{G} \in \{\mathcal{G}_1 = \mathcal{F}_1, \dots, \mathcal{G}_q = \mathcal{F}_q, \mathcal{G}_{q+1} = \mathcal{E}_1, \dots, \mathcal{G}_{q+m} = \mathcal{E}_m\}$.

B. The algorithm

Based on these gadget circuits we propose Algorithm 1 and provide a rigorous error analysis. We first consider the circuit for simulating the first segment. The indices of the sampled channel form a string $u_1 = s_{11}s_{12} \dots s_{1r} \in \{1, 2, \dots, q+m\}^r$ and corresponding Kraus operators are

$\{A_{1,1}, \dots, A_{1,n_1}\}, \dots, \{A_{r,1}, \dots, A_{r,n_r}\}$. By ignoring the extra qubit in step **3a**, the circuit W_1 performs the map

$$\begin{aligned} & |0\rangle_{\text{ctrl}}^{\otimes r} |0\rangle_{\text{sel}}^{\otimes r} |\psi\rangle \\ \mapsto & \sqrt{p^r} |0\rangle_{\text{ctrl}}^{\otimes r} \left(\sum_{j_1, \dots, j_r} |j_1, j_2, \dots, j_r\rangle_{\text{sel}} \prod_{k=r}^1 A_{j, j_k} |\psi\rangle \right) + |\perp\rangle, \end{aligned} \quad (20)$$

where $\text{tr}(|0\rangle\langle 0|_{\text{ctrl}}^{\otimes r} \otimes I_{\text{sel}}^{\otimes r} \otimes I) |\perp\rangle\langle \perp| = 0$. Notice that $p^r \geq (1-1/r)^r > 1/4$ by assuming $\tau \geq 2\lambda t$ and thus $R|0\rangle$ is a legal quantum state. With the extra qubit, we have

$$W_1 |\Psi\rangle = \frac{1}{2} |\Phi\rangle + \frac{\sqrt{3}}{2} |\Phi^\perp\rangle, \quad (21)$$

where

$$\begin{aligned} |\Psi\rangle &= |0\rangle |0\rangle_{\text{ctrl}}^{\otimes r} |0\rangle_{\text{sel}}^{\otimes r} |\psi\rangle, \\ |\Phi\rangle &= |0\rangle |0\rangle_{\text{ctrl}}^{\otimes r} \left(\sum_{j_1, \dots, j_r} |j_1, j_2, \dots, j_r\rangle_{\text{sel}} \prod_{k=r}^1 A_{j, j_k} |\psi\rangle \right). \end{aligned} \quad (22)$$

This enables us to perform oblivious amplitude amplification for isometries, which is F_1 . The following lemma restates Lemma 2 in [6] except that an index string is used to specify the sampled channels.

Lemma 4. *For any state $|\psi\rangle$ and index string $u_1 = s_{11}s_{12} \dots s_{1r} \in \{1, 2, \dots, q+m\}^r$, if we define*

$$F_1 = -W_1(I - 2P_1)W_1^\dagger(I - 2P_0)W_1, \quad (23)$$

where $P_0 = |0\rangle\langle 0| \otimes (|0\rangle\langle 0|_{\text{ctrl}}^{\otimes r} \otimes I_{\text{sel}}^{\otimes r} \otimes I)$ and $P_1 = |0\rangle\langle 0| \otimes (|0\rangle\langle 0|_{\text{ctrl}}^{\otimes r} \otimes (|0\rangle\langle 0|_{\text{sel}}^{\otimes r} \otimes I)$, then

$$\|F_1 |\Psi\rangle - |\Phi\rangle\|_2 \leq r(\delta \|\mathcal{L}\|_{\text{pauli}})^2, \quad (24)$$

where $|\Psi\rangle$ and $|\Phi\rangle$ are defined in Eq. (22)

Proof. To start with, $P_0 |\Phi^\perp\rangle = 0$. Then consider the circuit F_1 ,

$$\begin{aligned} \|F_1 |\Psi\rangle - |\Phi\rangle\|_2 &= \|(W_1 - 4W_1 P_1 W_1^\dagger P_0 W_1) |\Psi\rangle\|_2 \\ &= \|(I - 4P_1 W_1^\dagger P_0 W_1) |\Psi\rangle\|_2 \\ &= \|\Psi\rangle - 2P_1 W_1^\dagger |\Phi\rangle\|_2 \\ &= \|P_1(|\Psi\rangle - 2W_1^\dagger |\Phi\rangle)\|_2. \end{aligned} \quad (25)$$

Let $|\Psi^\perp\rangle = W_1^\dagger(\frac{\sqrt{3}}{2} |\Phi\rangle - \frac{1}{2} |\Phi^\perp\rangle)$, then $W_1^\dagger |\Phi\rangle = \frac{1}{2} |\Psi\rangle + \frac{\sqrt{3}}{2} |\Psi^\perp\rangle$, and

$$\|F_1 |\Psi\rangle - |\Phi\rangle\|_2 = \sqrt{3} \|P_1 |\Psi^\perp\rangle\|_2. \quad (26)$$

To bound $\|P_1 |\Psi^\perp\rangle\|_2$ we follow the analysis in [6, Lemma 3]. Consider the operator on the state register

$$Q = \text{tr}_{\text{anc}}(|0\rangle\langle 0| \otimes (|0\rangle\langle 0|_{\text{ctrl}}^{\otimes r} \otimes (|0\rangle\langle 0|_{\text{sel}}^{\otimes r}) W^\dagger P_0 W), \quad (27)$$

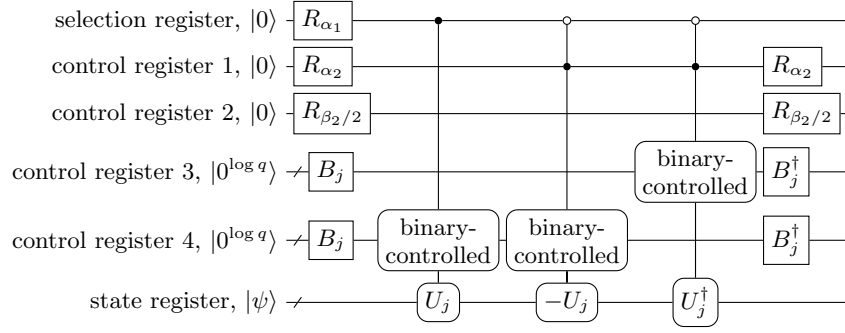


FIG. 3. Gadget circuit for simulating \mathcal{E}_j , where $B_j |0\rangle = \sum_{k=1}^q \sqrt{T_{jk}} |k\rangle$.

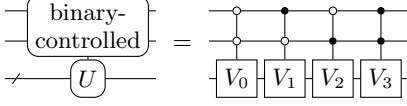


FIG. 4. Example of binary-controlled unitary matrices where the set of unitary matrices is $U = \{V_0, V_1, V_2, V_3\}$.

where we use tr_{anc} to denote partial trace operation that only leaves the state space. For any state $|\psi\rangle$ on the state register,

$$\begin{aligned} \langle \psi | Q | \psi \rangle &= \| P_0 W |0\rangle |0\rangle_{\text{ctrl}}^{\otimes r} |0\rangle_{\text{sel}}^{\otimes r} |\psi\rangle \|_2^2 \\ &= \frac{1}{4} \langle \Psi | \Psi \rangle, \end{aligned} \quad (28)$$

while

$$\begin{aligned} &| \langle \Psi | \Psi \rangle - 1 | \\ &= \left| \text{tr} \left[\left(\sum_{j_1, \dots, j_r} \prod_{l=1}^r A_{j_l, j_l}^\dagger \prod_{k=r}^1 A_{j_l, j_k} - I \right) |\psi\rangle \langle \psi| \right] \right| \\ &\leq \left\| \sum_{j_1, \dots, j_r} \prod_{l=1}^r A_{j_l, j_l}^\dagger \prod_{k=r}^1 A_{j_l, j_k} - I \right\|_1 \\ &\leq r(\delta \|\mathcal{L}\|_{\text{pauli}})^2. \end{aligned} \quad (29)$$

This suggests all eigenvalues of Q is about $\frac{1}{4}$, i.e. $\|Q - I/4\|_{\text{op}} \leq r(\delta \|\mathcal{L}\|_{\text{pauli}})^2/4$. Notice that

$$(Q - I/4) |\psi\rangle = \frac{\sqrt{3}}{4} (\langle 0 | \langle 0 |_{\text{ctrl}}^{\otimes r} \langle 0 |_{\text{sel}}^{\otimes r} \otimes I) |\Psi^\perp\rangle), \quad (30)$$

then

$$\begin{aligned} \|F_1 |\Psi\rangle - |\Phi\rangle\|_2 &= \sqrt{3} \|P_1 |\Psi^\perp\rangle\|_2 \\ &= \sqrt{3} \|(\langle 0 | \langle 0 |_{\text{ctrl}}^{\otimes r} \langle 0 |_{\text{sel}}^{\otimes r} \otimes I) |\Psi^\perp\rangle\|_2 \\ &= 4 \| (Q - I/4) |\psi\rangle \|_2 \\ &\leq 4 \|Q - I/4\|_{\text{op}} \\ &\leq r(\delta \|\mathcal{L}\|_{\text{pauli}})^2 = O(1/r). \end{aligned} \quad (31)$$

□

Algorithm 1 Randomized quantum algorithm for Lindbladian simulation

Require: Lindbladian represented by Hamiltonian H and jump operators $\{L_1, \dots, L_m\}$ with Pauli string decompositions, simulation time t and precision ϵ

1. Let $\tau = O(\lambda t)$, and $r = 2^{\lceil \log(\tau/\epsilon) \rceil}$, $\delta = t/(\tau r)$.
2. Initialize the selection registers and control registers to $|0\rangle^{\otimes r} |0\rangle^{\otimes r}$. Each selection register has 1 qubit and each control register has $2\lceil \log q \rceil + 1$ qubits.
3. For $k_1 = 1, \dots, \tau$,
 - (a) For $k_2 = 1, \dots, r$,
 - i. Sample a channel \mathcal{G} from $\{\mathcal{F}_1, \dots, \mathcal{F}_q, \mathcal{E}_1, \dots, \mathcal{E}_m\}$ with probability

$$\begin{cases} \Pr(\mathcal{G} = \mathcal{F}_l) = T_{0l}/\lambda, & l = 1, \dots, q \\ \Pr(\mathcal{G} = \mathcal{E}_j) = c_j^2/\lambda, & j = 1, \dots, m \end{cases}$$

and carry out $U_{\mathcal{G}, p}$ on the k_2 -th selection register, the k_2 -th control register and the state register. The index of the sampled channel is saved as $s_{k_1 k_2}$.

- (b) Denote the circuit formed in step **3a** in the k_1 -th iteration as W_{k_1} , which acts as a constant-time simulation. Add an extra qubit as a control register and a rotation gate $R|0\rangle = p^{-r/2}/2|0\rangle + \sqrt{1 - p^{-r}/4}|1\rangle$ on it.
- (c) Use oblivious amplitude amplification for isometries on W_{k_1} , with the target state being $|0\rangle |0\rangle^{\otimes r}$ on the control registers. The result is F_{k_1} .

4. Output the result circuit $V_s = F_\tau \dots F_2 F_1$.
-

Here $|\Phi\rangle$ is the purification of $\prod_{j=r}^1 \mathcal{G}_{s_{1j}}[|\psi\rangle \langle \psi|]$ for some arbitrary state $|\psi\rangle$, and $F_1 |\Psi\rangle$ is an $O(1/r)$ -approximation of it. This suggests F_1 simulates $\prod_{j=r}^1 \mathcal{G}_{s_{1j}}$ with error $O(1/r)$ on proper conditions, i.e.

$$\left\| \mathcal{M}_{u_1} - \prod_{j=r}^1 \mathcal{G}_{s_{1j}} \right\|_{\diamond} = O(1/r), \quad (32)$$

where u_1 is defined in Lemma 4, and \mathcal{M}_{u_1} is the quan-

tum channel implemented by F_1 on tracing out selection registers and control registers, with ancillary registers initialized to $|0\rangle|0\rangle_{\text{ctrl}}^{\otimes r}|0\rangle_{\text{sel}}^{\otimes r}$. Then

$$\begin{aligned} & \|\mathcal{M} - \mathcal{E}^r\|_{\diamond} \\ & \leq \sum_{u_1 \in \{1, \dots, q+m\}^r} p_{u_1} \left\| \mathcal{M}_{u_1} - \prod_{j=r}^1 \mathcal{G}_{s_{1j}} \right\|_{\diamond} \\ & = O(1/r), \end{aligned} \quad (33)$$

where \mathcal{M} is the quantum channel implemented by sampling M_{u_1} with probability $p_{u_1} = \prod_{j=r}^1 \Pr(\mathcal{G} = \mathcal{G}_{s_{1j}})$. If $s = u_1 \dots u_r = s_{11} \dots s_{r\tau}$ is sampled with probability $p_s = \prod_{j=\tau}^1 p_{u_j}$ and the selection registers and control registers are traced out, then channel $\mathcal{N} = \mathcal{M}^r$ is realized by Algorithm 1, and

$$\|\mathcal{N} - e^{\mathcal{L}t}\|_{\diamond} \leq \tau(\|\mathcal{M} - \mathcal{E}^r\|_{\diamond} + r\|\mathcal{E} - e^{\mathcal{L}\delta}\|_{\diamond}) = O(\epsilon). \quad (34)$$

By setting τ large enough, there is $\|\mathcal{N} - e^{\mathcal{L}t}\|_{\diamond} \leq \epsilon$.

We also analyze the total gate count in the algorithm. Figure 2 and 3 describe gadget circuits for simulating individual Hamiltonian and jump operators respectively. The former costs $O(n)$ elementary gates, and the latter costs $O(qn)$ elementary gates. Constant-time simulation circuit W_1 is composed of r gadget circuits and costs $O(rqn)$. Circuit $I - 2P_0$ and $I - 2P_1$ can be realized by multi-controlled Z gates on $O(r \log q)$ qubits, and they cost $O(r \log q)$ in total. Circuit F_1 costs $O(rqn)$ and V_s costs $O(\tau rqn) = O(qn\tau^2/\epsilon)$. Then we obtain Theorem 1.

V. SIMULATION VIA FRACTIONAL QUERY METHOD

In this section, we apply the Hamming-weight cutoff technique to reduce (t, ϵ) -dependence from $O(t^2/\epsilon)$ to $O\left(t \frac{\log(t/\epsilon)^2}{\log \log(t/\epsilon)}\right)$, at the cost of an extra $\tilde{O}(m)$ factor in the gate complexity. In Sec. V A, we briefly review the Hamming-weight cutoff technique and its application in Hamiltonian simulation, which is generalized to Lindbladian simulation in [6]. In Sec. V B, we provide a new probabilistic purification circuit of \mathcal{E} defined in Eq. (8) and shows that it meets the conditions for using the generalized Hamming-weight cutoff technique in [6]. We present the corresponding circuit design in Sec. V C. In the end, we combine them to propose Algorithm 2, and analyze its gate complexity in Sec. V D.

A. Hamming-weight cutoff

The Hamming-weight cutoff strategy is first proposed in [18] to simulate continuous-time query in discrete query model efficiently, and then applied in Hamiltonian simulation [17]. We will explain its intuition with an example of simulating e^{-iH} where H is both unitary and

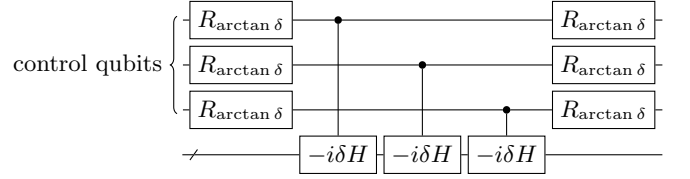


FIG. 5. Hamiltonian simulation circuit without Hamming-weight cutoff. The circuit performs $(I - i\delta H)^r$ on the state register when measuring $|0\rangle$ in all control qubits. An $r = 3$ example is presented.

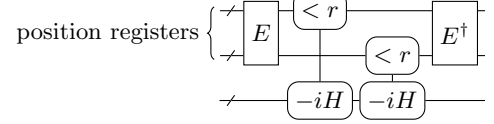


FIG. 6. Hamiltonian simulation circuit with Hamming-weight cutoff transformed from Figure 5. The circuit approximates $(I - i\delta H)^r$ on the state register when measuring $|r\rangle^{\otimes k}$ in all control qubits. A $k = 2$ example is presented.

Hermitian. We know that $e^{-i\delta H} = I - i\delta H + O(\delta^2)$, and $e^{-iH} = (I - i\delta H)^r + O(r\delta^2)$ where $r\delta = 1$. Therefore, with $O(r)$ call of $-iH$ we can simulate e^{-iH} with precision $O(1/r)$.

However, there is another way that approximates the original circuit and requires only $O(\frac{\log r}{\log \log r})$ calls of $-iH$, and the same precision remains $O(1/r)$. We expand polynomial $(I - i\delta H)^r$ with H as the variable and only consider terms with degree $\leq k$. Equivalently, we can equip each term with an r -bit string as its index, where "0" stands for taking I and "1" stands for taking $-i\delta H$, and only consider terms whose indices' Hamming weight is no more than k . Setting $k = O(\frac{\log \epsilon^{-1}}{\log \log \epsilon^{-1}})$ would introduce an extra error of no more than ϵ , therefore by setting $k = O(\frac{\log r}{\log \log r})$ the precision remains $O(1/r)$.

To obtain a succinct circuit that approximates e^{-iH} , we need a succinct representation of control qubits and the corresponding encoded rotation operator as well. Such an encoding scheme along with a gate-efficient encoded rotation operator E is proposed in [19]. The encoding scheme $\mathcal{C}_r^k : \mathcal{H}_2^{\otimes r} \rightarrow \mathcal{H}_{r+1}^{\otimes k}$ can be interpreted as a map from the original r -qubit Hilbert space to a smaller one, and this map maintains information on the subspace expanded by computational basis states with low Hamming weights. The encoded rotation operator is a unitary operator on the smaller Hilbert space such that

$$\left\| \mathcal{C}_r^k [(R_{\arctan \delta} |0\rangle)^{\otimes r}] - E \mathcal{C}_r^k [|0\rangle^{\otimes r}] \right\|_2 \leq \epsilon_{\text{enc}} \quad (35)$$

for some encoding error ϵ_{enc} . The encoded initial state $\mathcal{C}_r^k [|0\rangle^{\otimes r}] = |r\rangle^{\otimes k}$ can be efficiently prepared.

The Hamming-weight cutoff technique is generalized to Lindbladian simulation in [6]. It turns out that, with minimal modifications, this generalized method can be applied to our method.

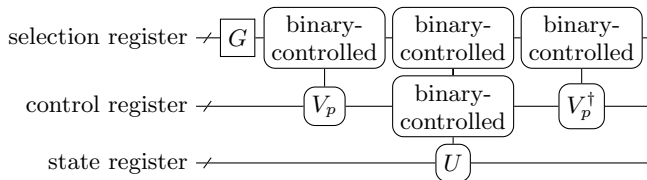


FIG. 7. Probabilistic purification circuit proposed in [6]. The Hamming-weight cutoff technique applies to circuits that both have the same structure and satisfy the amplitude condition.

B. Fragment simulation gadget

Our target is to implement the probabilistic purification circuit of \mathcal{E} that is suitable for the generalized Hamming-weight cutoff technique.

To start with, the probabilistic purification $U_{\mathcal{E},p}$ can be implemented efficiently by gadgets in Figure 2 and 3, in the style presented in Figure 12. Next, we rearrange the circuit, fitting into the four-part structure: selection preparation G , control preparation V_p , multiplexed unitary V_c , and control preparation inverse V_p^\dagger , which is called the structure condition. This is possible since any controlled gates commute as long as they are controlled by different binary strings on the first selection register, as shown in Figure 11. We can also simplify these controlled gates by some simple circuit synthesis techniques (see Figure 12). Precise construction is given in Figure 13 and 14. The resulting circuit in Figure 16 is a probabilistic purification circuit for \mathcal{E} with probability p that is suitable for the generalized Hamming-weight cutoff technique. Next, we confirm this by the following amplitude argument. Intuitively, there is a subspace such that any state in this subspace leads to performing identity in the multiplexed unitary gate V_c . If the state after the preparation circuits V_p, G "mostly" falls into this trivial subspace, then it can be compressed, and the number of multiplexed unitary gates can be reduced. In the following, we prove that, for our construction in Figure 16, this state indeed meets this condition. Consider the state of all the selection and control registers. The state right before the multiplexed unitary gate in Figure 16 is

$$\sum_{l=1}^q \sqrt{\Pr(\mathcal{G} = \mathcal{F}_l)} |l, 0\rangle_{\text{sel}} |\alpha, \beta_1/2, 0, 0\rangle_{\text{ctrl}} + \sum_{j=1}^m \sqrt{\Pr(\mathcal{G} = \mathcal{E}_j)} |q+j, \alpha_1\rangle_{\text{sel}} |\alpha_2, \beta_2/2, B_j, B_j\rangle_{\text{ctrl}}, \quad (36)$$

where $|\theta\rangle = R_\theta |0\rangle$ for some angle θ , $|B_j\rangle = B_j |0\rangle$ for $j = 1, \dots, m$, and β_1, β_2 are angles shown in Figure 2 and 3, respectively. Consider a subspace s_I formed by a projection

$$P_I = (I \otimes |0\rangle\langle 0|)_{\text{sel}} \otimes (|0\rangle\langle 0| \otimes I \otimes I \otimes I)_{\text{ctrl}}.$$

All states in this subspace lead to performing identity I

in the following multiplexed unitary gate V_c . If we measure the state in Eq. (36) by a projective measurement $\{P_I, I - P_I\}$, the probability that we obtain the outcome corresponding to P_I is

$$\begin{aligned} p_I &= \frac{\sum_{l=1}^q \Pr(\mathcal{G} = \mathcal{F}_l)}{1 + \tan \alpha} + \frac{\sum_{j=1}^m \Pr(\mathcal{G} = \mathcal{E}_j)}{(1 + \tan \alpha_1)(1 + \tan \alpha_2)} \\ &\geq \frac{1}{(1 + \tan \alpha_1)(1 + \tan \alpha_2)} \\ &\geq 1 - \frac{3}{2} \lambda \delta = 1 - \frac{3}{2r}. \end{aligned} \quad (37)$$

This is of the same scaling as in [6]. By applying the same Chernoff bound analysis we conclude that $h = O\left(\frac{\log r}{\log \log r}\right)$ multiplexed unitary gates do not change the order of the error, which remains $O(1/r)$.

A key technical contribution of [6] is a compression scheme suitable for circuits of the above kind. More precisely, for a probabilistic purification circuit with the same structure as Figure 7 and satisfying the amplitude argument, there exists an encoding scheme $\mathcal{C} : (\mathcal{H}_{\text{sel}} \otimes \mathcal{H}_{\text{ctrl}})^{\otimes r} \rightarrow \mathcal{H}_{r+1}^{\otimes h} \otimes (\mathcal{H}_{\text{sel}} \otimes \mathcal{H}_{\text{ctrl}})^{\otimes h}$ and an encoded rotation operator E_{r_0} such that

$$\left\| \mathcal{C} \left[(V_p(G \otimes I) |0, 0\rangle^{\otimes r}) - E_{r_0} \mathcal{C} \left[|0, 0\rangle^{\otimes r} \right] \right\|_2 \leq \epsilon_{\text{enc}} \quad (38)$$

for some encoding error ϵ_{enc} . For different probabilistic purification circuits, only E_{r_0} would be different. In [6], the construction of E_{r_0} specified by the channel LCU circuit is described.

With the desired probabilistic purification circuit and efficient construction of E_{r_0} specified by this circuit, we can apply the technique in [6] to achieve the same $O(\text{tpoly} \log(t/\epsilon))$ dependence.

C. Encoded rotation operator

In this subsection, we give a concrete implementation of the encoded rotation operator suitable for our purification circuit.

We consider the constant-time simulation circuit W in Figure 8. The circuit W is almost the same as W_{k_1} in step 3b of Algorithm 1, except that the sampling process is replaced with a deterministic circuit in Figure 16. It has r gadget circuits and corresponding r selection and control registers.

Consider the computational basis of all r ancillary registers $|l_1, k_1\rangle \dots |l_r, k_r\rangle$, where l_i and k_i label the selection and control register in the i -th gadget, respectively. The encoding scheme [6] compress this state to

$$|g_1, \dots, g_h\rangle |l_{i_1}, k_{i_1}\rangle \dots |l_{i_h}, k_{i_h}\rangle$$

where $|l_{i_1}, k_{i_1}\rangle \dots |l_{i_h}, k_{i_h}\rangle$ records the first h selection and control registers that is not in s_I , and $|g_1, \dots, g_h\rangle$ encodes their position, where $h = O\left(\frac{\log r}{\log \log r}\right)$ is enough

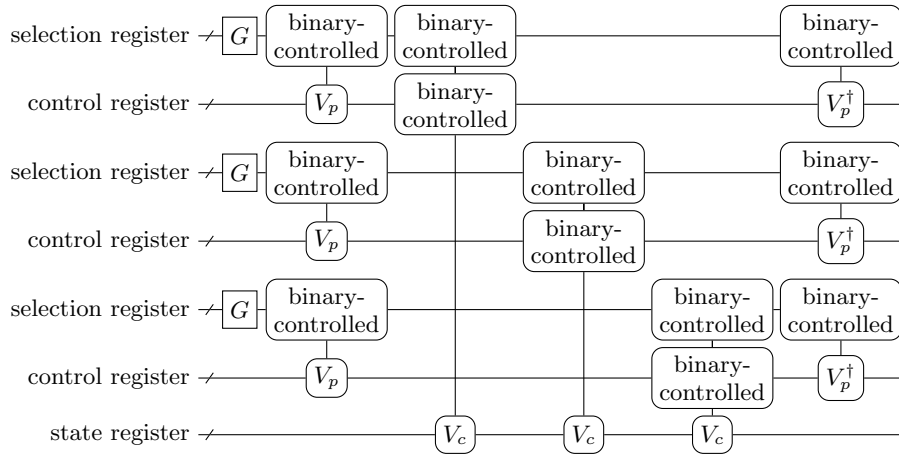


FIG. 8. The constant-time simulation circuit W . An $r = 3$ example is presented.

according to the Hamming-weight cutoff technique. The construction of E_{ro} consists of two parts: a standard encoded rotation operator [19] on the position registers $|g_1, \dots, g_h\rangle$, followed by modified preparation circuits $V'_p(G' \otimes I)$. We only need to compose the latter part according to our probabilistic purification circuit in Figure 16. The modified version we need is

$$V'_p(G' \otimes I) |0, 0\rangle = \frac{1}{\lambda_*} (I - P_I) V_p(G \otimes I) |0, 0\rangle \quad (39)$$

where $\lambda_* = \|(I - P_I) V_p(G \otimes I) |0, 0\rangle\|_2$.

The modified version can be done efficiently. Let $x_\theta = (1 + \tan \theta)^{-1}$ for some θ . The state we try to prepare is

$$\sum_{l=1}^q x_l |l, 0\rangle_{\text{sel}} |\xi\rangle_{\text{ctrl}} + \sum_{j=1}^m \sum_{\substack{b_1, b_2 \in \{0, 1\} \\ b_1 b_2 \neq 0}} x_{j, b_1, b_2} |q + j, b_1\rangle_{\text{sel}} |\nu_j\rangle_{\text{ctrl}}. \quad (40)$$

where

$$|\xi\rangle = |1, \beta_1/2, 0, 0\rangle, \quad (41)$$

$$x_l = \sqrt{\Pr(\mathcal{G} = \mathcal{F}_l) \frac{1 - x_\alpha}{\lambda_*}},$$

for $l = 1, \dots, q$, and

$$|\nu_j\rangle = |b_2, \beta_2/2, B_j, B_j\rangle, \quad (42)$$

$$x_{j, b_1, b_2} = \sqrt{\Pr(\mathcal{G} = \mathcal{E}_j) \frac{(1 - x_{\alpha_1})^{b_1} (1 - x_{\alpha_2})^{b_2}}{\lambda_*}},$$

for $j = 1, \dots, m, b_1 = 0, 1, b_2 = 0, 1$. Circuit G' prepares the state $\sum_{l=1}^q x_l |l, 0\rangle_{\text{sel}} + \sum_{j=1}^m \sum_{\substack{b_1, b_2 \in \{0, 1\} \\ b_1 b_2 \neq 0}} x_{j, b_1, b_2} |q + j, b_1\rangle_{\text{sel}}$, and costs at most $O(m + q)$ elementary gate. In V'_p , controlled rotation gates from V_p need modification, and the rest

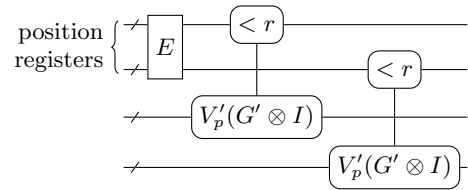


FIG. 9. The encoded rotation operator E_{ro} . It consists of two parts: a standard encoded rotation operator E [19] on the position registers $|g_1, \dots, g_h\rangle$, followed by modified preparation circuits $V'_p(G' \otimes I)$. An $h = 2$ example is shown.

gates (controlled B_j gates) stay the same. The resulting circuit is shown in Figure 15, and its gate cost remains $O(mq)$.

We also need a circuit V'_c that corresponds to V_c in the original representation. V'_c has a more straightforward construction, by simply adding the condition $g_i < r$ to the original V_c .

D. The algorithm

In summation, we propose Algorithm 2, which realizes an exponential speedup in the precision parameter compared to Algorithm 1, at the cost of an extra $O(m)$ factor in gate complexity introduced by a multiplexed operation on $U_{\mathcal{G}_j, p}, j = 1, \dots, m + q$.

For analysis of the total gate count, we consider the circuit for simulating a single segment, i.e. the circuit created from one loop of step 3. It consists of $O(1)$ encoded rotation operators E_{ro} , $O(h)$ multiplexed unitary gates V'_c , and two reflection operators. The first part of E_{ro} can be implemented with $O(h(\log r + \log \log \epsilon_2^{-1}))$ elementary gates [19], where ϵ_2 is the error introduced by an approximation of the encoding scheme and we take $\epsilon_2 = O(1/r)$. The second part consists of h copies of V'_p and G' and each costs $O(mq)$ elementary gates. Therefore, the cost of the encoded rotation operator E_{ro} is $O(h(\log r + mq))$. Mul-

VI. EXAMPLES

Algorithm 2 Quantum algorithm for Lindbladian simulation with exponential precision improvement

Require: Lindbladian represented by Hamiltonian H and jump operators $\{L_1, \dots, L_m\}$ with Pauli string decomposition, simulation time t and precision ϵ

1. Let $\tau = O(\lambda t)$, $r = 2^{\lceil \log(\tau/\epsilon) \rceil}$, $\delta = t/(\tau r)$ and $h = O(\frac{\log r}{\log \log r})$.
2. Initialize the position register, selection registers, and control registers to $|r, \dots, r\rangle (|0\rangle |0\rangle)^{\otimes h}$. The position register is composed of h subregisters and each has $\log r$ qubits. Each selection register has $\lceil \log(m+q) \rceil + 1$ qubit and each control register has $2\lceil \log q \rceil + 2$ qubits.
3. For $k_1 = 1, \dots, \tau$,
 - (a) Carry out the encoded rotation operator E_{r_0} .
 - (b) For $k_2 = 1, \dots, h$,
 - i. Carry out V'_c controlled on the k_2 -th position subregister, k_2 -th selection register, the k_2 -th control register.
 - (c) Carry out the encoded rotation operator $E_{r_0}^\dagger$.
 - (d) Reflect about the subspace where the state of the position register is $|r\rangle^{\otimes h}$ and the state of all control registers is $|0\rangle$.
 - (e) Carry out the encoded rotation operator E_{r_0} .
 - (f) Carry out the inverse of the circuit created in step **3b**.
 - (g) Carry out the encoded rotation operator $E_{r_0}^\dagger$.
 - (h) Reflect about the subspace where the state of the position register is $|r\rangle^{\otimes h}$ and the state of all selection and control registers is $|0\rangle$.
 - (i) Carry out the circuit created from step **3b**.
 - (j) Carry out the encoded rotation operator E_{r_0} .
4. Output the result circuit V .

tiplexed unitary gate V'_c consists of $O(mq)$ Pauli strings controlled on $O(\log r + \log(mq))$ qubits, and their cost is $O(mq(n + \log r + \log(mq)))$. The reflection operators can be viewed as Z gate controlled on at most $O(h(\log r + \log(mq)))$ qubits and their cost is $O(h(\log r + \log(mq)))$. Therefore, the circuit for simulating one segment has a cost of $O(h(\log r + mq) + mqh(n + \log r + \log(mq)) + h(\log r + \log(mq))) = O(mqh(\log r + n + \log(mq)))$. There are τ segments and $h = O(\frac{\log r}{\log \log r})$, $r = O(\tau/\epsilon)$, and the gate complexity of V is

$$O\left(mq\tau \frac{(\log(mq\tau/\epsilon) + n) \log(\tau/\epsilon)}{\log \log(\tau/\epsilon)}\right), \quad (43)$$

which leads to Theorem 2.

The number of jump operators m in \mathcal{L} of an n -qubit system can be up to 4^n , and therefore the removal of m -dependence can be an exponential improvement. We consider two examples to demonstrate such improvements. In the first example, the dissipation is given by a depolarizing channel, and the Hamiltonian has a constant Pauli norm and can be expressed as the sum of $\text{poly}(n)$ Pauli strings. The other example is the evolution of the dissipative quantum XY model [20]. In both scenarios, we obtain better results than the previous best gate-based algorithm [6].

For scenario 1 listed in Table II, we first consider the simulation of the depolarizing channel. Consider the following state

$$\rho(t) = \Delta_{\lambda(t)}(\rho(0)) = (1 - \lambda(t))\rho(0) + \lambda(t)\frac{I}{2^n}, \quad (44)$$

where $\lambda(t) = 1 - e^{-t}$. By setting different t , we are able to simulate $\Delta_\lambda, \lambda \in [0, 1]$ via simulating $\rho(t)$. We assert that $\rho(t)$ can be derived from $\rho(0)$ via Lindbladian simulation. Notice that

$$\begin{aligned} \frac{d\rho(t)}{dt} &= -\rho(t) + \frac{I}{2^n} \\ &= 4^{-n} \sum_{P \in \text{Pauli}(n)} \left(P\rho(t)P^\dagger - \frac{1}{2} \{P^\dagger P, \rho(t)\} \right) \\ &= \mathcal{L}_0(\rho(t)), \end{aligned} \quad (45)$$

where $\text{Pauli}(n) = \{I, X, Y, Z\}^{\otimes n}$. This suggests $\rho(t) = e^{\mathcal{L}_0 t} \rho(0)$. Then we combine it with the given Hamiltonian H ,

$$\begin{aligned} \frac{d\rho(t)}{dt} &= -i[H, \rho] + 4^{-n} \sum_{P \in \text{Pauli}(n)} \left(P\rho(t)P^\dagger - \frac{1}{2} \{P^\dagger P, \rho(t)\} \right) \\ &= \mathcal{L}(\rho(t)), \end{aligned} \quad (46)$$

and obtain a Lindbladian \mathcal{L} with a Hamiltonian and 4^n jump operators $\{\frac{P}{2^n} | P \in \text{Pauli}(n)\}$. In this scenario, the Lindbladian simulation has the following parameters,

$$\begin{aligned} m &= 4^n, \\ q &= \text{poly}(n), q_0 = 1 \\ \|\mathcal{L}\|_{\text{pauli}} &= O(1) + 4^n (2^{-n})^2 = O(1), \\ t &= \ln\left(\frac{1}{1-\lambda}\right), \\ \epsilon &= O(1). \end{aligned} \quad (47)$$

where \mathcal{L}_0 can be described as linear combination of q_0 Pauli strings.

In scenario 2, we consider a Lindbladian with Hamiltonian $H = -J \sum_{(i,j) \in E} (X_i X_j + Y_i Y_j)$ and n jump operators $\{Z_1, Z_2, \dots, Z_n\}$. By fully connected topology we

refer to $E = \{(i, j) | 1 \leq i < j \leq n\}$. We also set interaction strength to $J = -1$. The parameters of the Lindbladian simulation are

$$\begin{aligned} m &= n, \\ q &= \frac{n(n-1)}{2}, \\ \|\mathcal{L}\|_{\text{pauli}} &= n(n-1) + n = n^2, \\ t &= n, \\ \epsilon &= O(1). \end{aligned} \quad (48)$$

By substituting parameters in Theorem 2 and 1, we obtain results in Table II.

Algorithm	Scenario 1	Scenario 2
Algorithm 1	$O(n)$	$O(n^7)$
Algorithm 2	$O(\text{poly}(n)2^{2n})$	$O(n^6 \log n)$
Channel LCU scheme [6]	$O(\text{poly}(n)2^{4n})$	$O(n^9 \log n)$

TABLE II. Comparison of previous best gate-based algorithm [6] for Lindbladian simulation and our algorithms. In the first scenario, we consider "depolarized" Hamiltonian simulation on n qubits, with constant precision ϵ and constant depolarizing rate λ . In the second scenario, we consider the simulation of the n -qubit dissipative quantum XY model (as defined in [20]) with full connection topology, interaction strength $J = -1$, time $t = n$ and constant precision. Notice that for scenario 1, we use a strengthened version of Theorem 1, where the gate count can be reduced to $O\left(\frac{q_0 n \tau^2}{\epsilon}\right)$, where q_0 is the maximum Pauli string number for jump operators only.

VII. DISCUSSION AND CONCLUSION

In this paper, we have proposed two quantum algorithms for simulating Lindbladian evolution. Our key contribution is the introduction of a new approximation channel inspired by the quantum trajectory method. Using this approximation channel, we propose Algorithm 1, which remains efficient even with an arbitrarily large number of jump operators. Algorithm 2 combines the approximation channel with the fractional query method, achieving a near-optimal (t, ϵ) -dependence at the cost of an (m, q) -dependence of $\tilde{O}(mq)$. Despite this, Algorithm 2 outperforms previous algorithms that are based on linear combinations of Pauli operators [6], which have the same (t, ϵ) -dependence but an (m, q) -dependence of $\tilde{O}(m^2 q^2)$. Our algorithm allows simulation with more jump operators and achieves exponentially higher precision.

Additionally, [7] proposed a block-encoding-based quantum algorithm for Lindbladian simulation. When the block-encoding part is implemented using the LCU method, it has the same asymptotic gate complexity as Algorithm 2. While this suggests that Algorithm 2 is not the only state-of-the-art algorithm for Lindbladian

simulation, our results still provide valuable insights into the structured LCU construction. Given the complicated construction of Kraus operators in [7], a detailed comparison between our method and [7] would be of great interest.

Several open questions remain. It would be interesting to explore the possibility of combining the merits of Algorithms 1 and 2. Specifically, we wonder if it is possible to develop a quantum algorithm for Lindbladian simulation that achieves an ϵ -dependence of $O(\log \epsilon^{-1})$ while being independent of m concerning gate complexity. A closely related open problem in Hamiltonian simulation is to achieve an ϵ -dependence of $O(\log \epsilon^{-1})$ while being independent of q (the number of Pauli strings in the Hamiltonian). Additionally, establishing a lower bound on the (m, q, t, ϵ) -dependence for Lindbladian simulation or the (q, t, ϵ) -dependence for Hamiltonian simulation would be of significant interest.

ACKNOWLEDGMENTS

We gratefully acknowledge Benjamin Desef, the author of the `yquant` LaTeX package, for providing instructions on drawing specific complex quantum gates. We thank Chunhao Wang for insightful discussions. This work was supported in part by the National Natural Science Foundation of China Grants No. 62325210, 62272441, 12204489, 62301531, and the Strategic Priority Research Program of Chinese Academy of Sciences Grant No. XDB28000000.

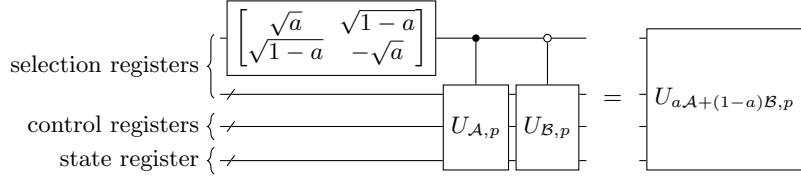


FIG. 10. Probabilistic purification circuit for the mixed channel $a\mathcal{A} + (1 - a)\mathcal{B}$ for $a \in [0, 1]$, given individual channels' probabilistic purification with the same probability.

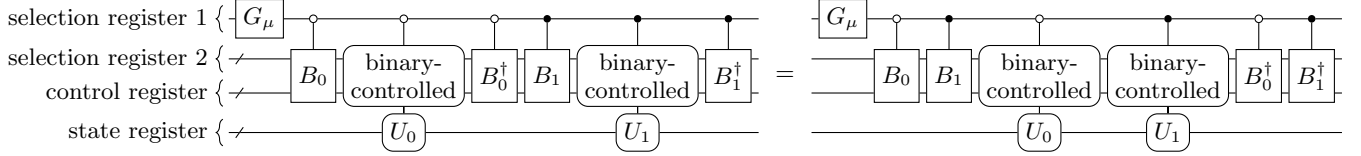


FIG. 11. Probabilistic purification circuit for the mixed channel can be rearranged to maintain the structure of binary-controlled unitary matrices.

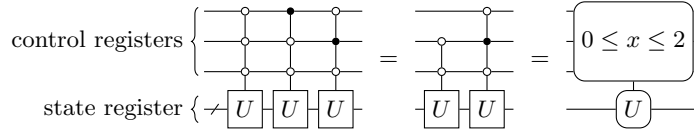


FIG. 12. Gates of the same kind but controlled on different conditions can be combined.

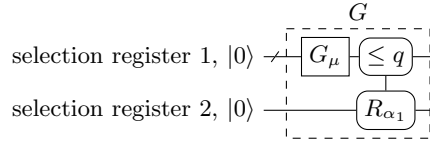


FIG. 13. Selection preparation circuit G , which prepares probability distribution.

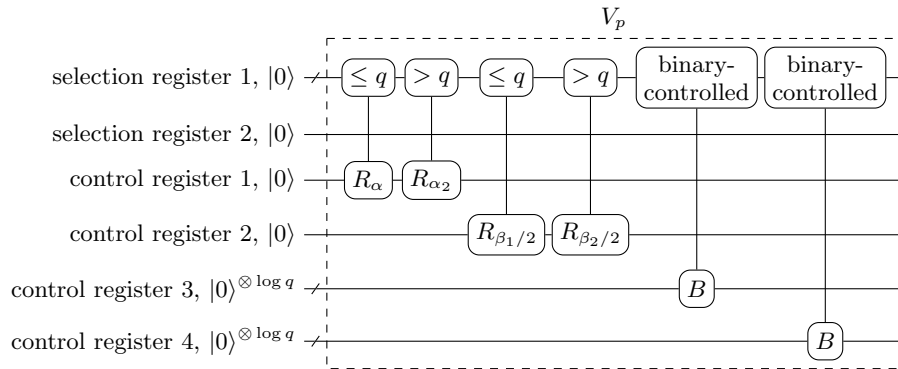
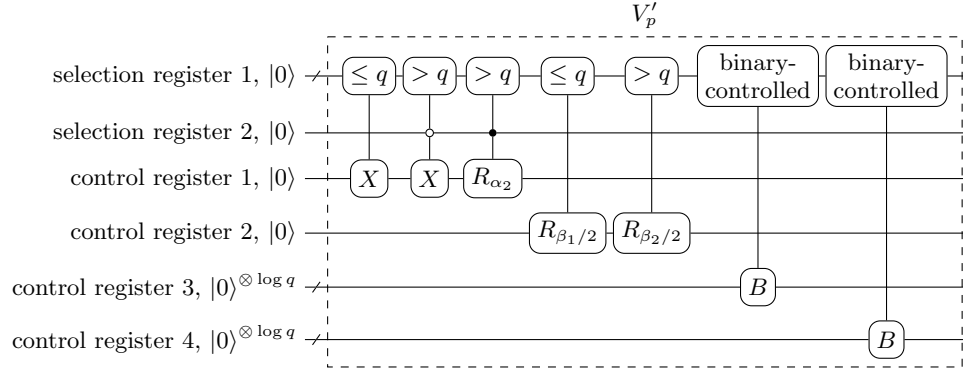
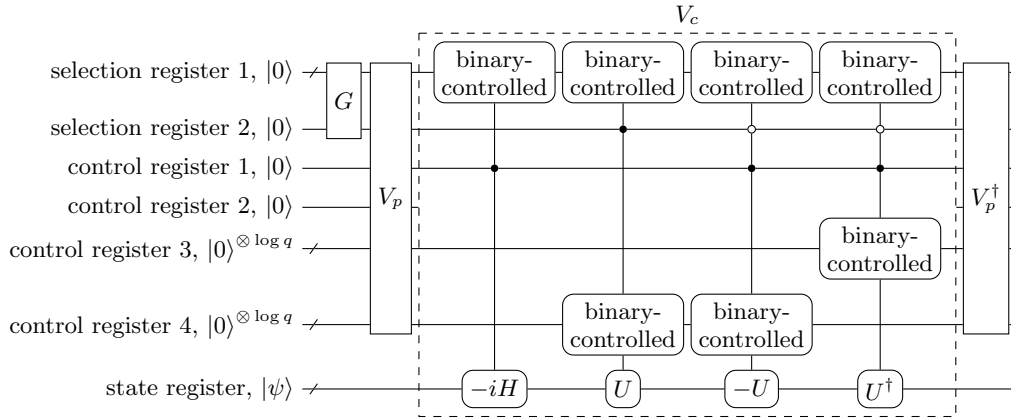


FIG. 14. Control preparation circuit V_p for mixing linear coefficients.

FIG. 15. Encoded control preparation circuit V'_p .FIG. 16. Probabilistic purification circuit for the mixed channel \mathcal{E} suitable for Hamming-weight cutoff.

-
- [1] R. P. Feynman, *International Journal of Theoretical Physics* **21**, 467 (1982).
- [2] A. Nitzan, *Chemical Dynamics in Condensed Phases: Relaxation, Transfer and Reactions in Condensed Molecular Systems* (Oxford University Press, 2006).
- [3] V. May and O. Kühn, *Charge and Energy Transfer Dynamics in Molecular Systems* (John Wiley & Sons, Ltd, 2011).
- [4] U. Weiss, *Quantum Dissipative Systems*, 4th ed. (WORLD SCIENTIFIC, 2012) <https://www.worldscientific.com/doi/pdf/10.1142/8334>.
- [5] Z. Chen, Y. Lu, H. Wang, Y. Liu, and T. Li, “Quantum langevin dynamics for optimization,” (2024), arXiv:2311.15587.
- [6] R. Cleve and C. Wang, in *44th International Colloquium on Automata, Languages, and Programming (ICALP 2017)*, Leibniz International Proceedings in Informatics (LIPIcs), Vol. 80, edited by I. Chatzigiannakis, P. Indyk, F. Kuhn, and A. Muscholl (Schloss Dagstuhl – Leibniz-Zentrum für Informatik, Dagstuhl, Germany, 2017) pp. 17:1–17:14.
- [7] X. Li and C. Wang, in *50th International Colloquium on Automata, Languages, and Programming (ICALP 2023)*, Leibniz International Proceedings in Informatics (LIPIcs), Vol. 261, edited by K. Etessami, U. Feige, and G. Puppis (Schloss Dagstuhl – Leibniz-Zentrum für Informatik, Dagstuhl, Germany, 2023) pp. 87:1–87:20.
- [8] M. Pocrnic, D. Segal, and N. Wiebe, “Quantum simulation of lindbladian dynamics via repeated interactions,” (2024), arXiv:2312.05371 [quant-ph].
- [9] Z. Ding, X. Li, and L. Lin, *PRX Quantum* **5**, 020332 (2024).
- [10] D. Patel and M. M. Wilde, *Open Systems & Information Dynamics* **30**, 2350010 (2023), <https://doi.org/10.1142/S1230161223500105>.
- [11] D. Patel and M. M. Wilde, *Open Systems & Information Dynamics* **30**, 2350014 (2023), <https://doi.org/10.1142/S1230161223500142>.
- [12] E. Campbell, *Phys. Rev. Lett.* **123**, 070503 (2019).
- [13] J. Dalibard, Y. Castin, and K. Mølmer, *Phys. Rev. Lett.* **68**, 580 (1992).
- [14] K. Mølmer, Y. Castin, and J. Dalibard, *J. Opt. Soc. Am. B* **10**, 524 (1993).
- [15] R. Dum, P. Zoller, and H. Ritsch, *Phys. Rev. A* **45**, 4879 (1992).
- [16] A. J. Daley, *Advances in Physics* **63**, 77 (2014).
- [17] D. W. Berry, A. M. Childs, R. Cleve, R. Kothari, and R. D. Somma, in *Proceedings of the Forty-Sixth Annual ACM Symposium on Theory of Computing, STOC '14* (Association for Computing Machinery, New York, NY, USA, 2014) p. 283–292.
- [18] R. Cleve, D. Gottesman, M. Mosca, R. D. Somma, and D. Yonge-Mallo, in *Proceedings of the Forty-First Annual ACM Symposium on Theory of Computing, STOC '09* (Association for Computing Machinery, New York, NY, USA, 2009) p. 409–416.
- [19] D. W. Berry, R. Cleve, and S. Gharibian, *Quantum Info. Comput.* **14**, 1–30 (2014).
- [20] H.-Y. Liu, X. Lin, Z.-Y. Chen, C. Xue, T.-P. Sun, Q.-S. Li, X.-N. Zhuang, Y.-J. Wang, Y.-C. Wu, M. Gong, and G.-P. Guo, “Simulation of open quantum systems on universal quantum computers,” (2024), arXiv:2405.20712.